King Saud University

Arabian Journal of Chemistry

www.ksu.edu.sa
www.sciencedirect.com

ORIGINAL ARTICLE

Phillyrin ameliorated collagen-induced arthritis through inhibition of NF-κB and MAPKs pathways in fibroblast-like synoviocytes

Gang Chen, Yuhang Mao, Jing Wang, Junnan Zhou, Li Diao, Sirui Wang, Wenjuan Zhao, Xinyi Zhu, Xiaolu Yu, Fuli Zhao, Xuan Liu, Mei Liu [*]

Jiangsu Key Laboratory for Molecular and Medical Biotechnology and College of Life Sciences, Nanjing Normal University, Nanjing 210023, China

Abstract   The discovery of alternative medicines with less adverse effects is extremely urgent for rheumatoid arthritis (RA). Phillyrin (Phil), the predominant lignan glycoside of *Forsythia suspensa*, has been reported to exert several pharmacological effects, such as antivirus, anti-inflammation, anti-oxidation, anti-obesity, and antipyretic activity. However, the effect of Phil on RA remains unknown. In this study, We utilized both *in vivo* collagen-induced arthritis (CIA) rat models and *in vitro* TNFα-induced fibroblast-like synoviocytes (FLSs) to study the inhibitory effects of Phil on RA. The *in vivo* studies revealed that Phil treatment effectively ameliorated synovial inflammation and bone erosion in CIA rats. The *in vitro* studies demonstrated that Phil could significantly suppress the proliferation and migration of arthritic FLSs. In addition, treatment with Phil resulted in decreased mRNA expression of proinflammatory cytokines including *TNFα*, *IL-1β*, *IL-6*, *IL-8* and *MMP9*. Molecular mechanistic investigations revealed that the suppressive effects of Phil were mediated by blockade of the MAPK (ERK, p38, and JNK) and NF-κB pathways. Taken together, our findings suggest that Phil has an anti-arthritic effect in CIA rats by inhibiting the pathogenic characteristic of arthritic FLSs throught suppression of NF-κB and MAPKs signaling pathways. These results demonstrate the potential of Phil as a novel therapeutic agent for the treatment of RA.

1. Introduction

Rheumatoid arthritis (RA) is a chronic disease characterized by systemic invasive arthritis, mainly involving joint synovitis and bone destruction (Klareskog et al., 2009). Despite the involvement of multi-ple cell types in the pathogenesis of RA, emerging evidence highlights the critical role of fibroblast-like synoviocytes (FLSs) as significant contributors and effectors of the disease. Over-activated RA FLSs exhibit increased proliferation and invasion, resistance to apoptosis, and secrete proinflammatory cytokines (Pallavi et al., 2019). The

---

[*] Corresponding author.
  E-mail address: meiliunj@163.com (M. Liu).

histological and radiological damages in RA patients and rodent models proved to be closely related to these destructive properties of FLSs (Tolboom et al., 2005; Ralph and Morand, 2008; Laragione et al., 2010). Therefore, therapies targeting RA FLSs may represent the most promising option for treating RA patients.

Currently, the goal of clinical treatment for RA has shifted from merely relieving joint swelling to preventing joint bone destruction, achieving disease alleviation, and ultimately enhancing the quality of life of patients (Khraishi, 2014). Nonsteroidal anti-inflammatory drugs (NSAIDs) and glucocorticoids (GC) are commonly used for pain relief or inflammation control, but their therapeutic effects are limited to clinical symptom relief and cannot effectively halt the progression of the disease (O'Dell and James, 2004; Scott, 2012; Khraishi, 2014). Disease-modifying anti-rheumatic drugs (DMARDs) and biologic agents have been shown to delay or control RA progression, but long-term use of these drugs may cause serious adverse events (Putte et al., 2003). Considering the limitations and potential risks associated with current RA treatments, natural compounds are emerging as a viable alternative for therapy due to their favorable curative effects and low toxicity.

Forsythiae Fructus (Lianqiao in China), the fruit of *Forsythia suspensa* (Thunb.) *Vahl* (Oleaceae), is known as a widely used heat-clearing and detoxifying herb because of its characteristics of slightly cold nature, bitter flavor, and lung meridian distribution (Pharmacopoeia Commission of PRC, 2015). The heat-clearing action of *F. suspensa* is attributed to the presence of lignans and phenylethanoid glycosides, which possess antioxidant and anti-inflammatory properties (Wang et al., 2018). Phillyrin (Phil) is the predominant lignan glycoside isolated from *F. suspensa*. and possesses a variety of pharmacological effects, including antivirus, anti-oxidation, anti-obesity, and anti-inflammatory activity (Zhang et al., 2014; Yang et al., 2017; Du et al., 2020; Zhang et al., 2020). Our previous study showed that Phil could inhibit osteoclast differentiation and bone-resorption activity, and thereby prevent LPS-induced osteolysis (Wang et al., 2019). Bone erosion is a critical histopathological feature of RA, and osteoclasts play a significant role in this destructive process. In addition, previous reports have demonstrated that Phil can inhibit the activation of NF-κB and MAPKs in various cell types (Zhong et al., 2013; Zhang et al., 2019; Lu et al., 2020). These pathways have been shown to be critical for the pathogenesis of RA (Müller-Ladner et al., 2005; Zhou et al., 2007; Ralph and Morand, 2008; Noss et al., 2011). Given the aforementioned evidence, it is plausible that Phil could serve as a promising therapeutic candidate for RA. Therefore, in this study, we aimed to investigate the protective effect of Phil on type II collagen-induced arthritis (CIA) in Wistar rats and its potential to inhibit the pathogenic characteristics of arthritic FLSs, while uncovering its underlying molecular mechanisms.

2. Methods and materials

2.1. Animals

Female Wistar rats (160–180 g) were obtained from Shanghai Slac Laboratory Animal Co., Ltd. (Shanghai, China). These animals were housed in specific pathogen-free (SPF) conditions bred with water and food accessible. The animal experiments were carried out in accordance with the protocol by the Experimental Committee of Nanjing Normal University (IACUC-20201203).

2.2. Preparation of CIA animal model and treatment with Phil

To establish the rat CIA model, we followed the previously described protocol (Qiu et al., 2018), which involved an intra-dermal injection of a 1:1 emulsion of chicken CII (1 mg/ml, Sigma, Saint Louis, MO, USA) and CFA containing Mycobacterium butyricum (Sigma, Saint Louis, MO, USA) in Wistar rats. On day 7, CII (0.5 mg/ml) emulsified with IFA (Sigma, Saint Louis, MO, USA) were subcutaneously boosted in these animals. The rats were immunized with 0.9% saline in the same way as healthy controls. In this study, a total of 42 rats were purchased, with 7 used as healthy controls and the remaining 35 used for CIA modeling. Our laboratory has achieved an approximate 80% success rate in constructing CIA models. Specifically, in this study, 28 out of 35 rats were successfully modeled for CIA. Once reaching an arthritis index score $\geq$ 2, the 28 CIA rats were randomly divided into various groups (n = 7): vehicle-treated CIA group (CIA rats treated with 0.9% saline); MTX-treated group (CIA rats treated with 3 mg·kg^{-1} MTX); Phil-treated groups (CIA rats treated with 10 and 20 mg·kg^{-1} Phil, respectively). Notably, Phil or 0.9% saline was intraperitoneally given once a day for up to 14 days. Phil (HPLC $\geq$ 98%, $C_{27}H_{34}O_{11}$, MW: 534.55, Catalog #: L-010) was purchased from Must Bio-Technology Co., Ltd. (Sichuan, China). Its dosage was determined based on our preliminary experiments and previous reports (Qu et al., 2010; Zhong et al., 2013; Cheng et al., 2017; Wang et al., 2019). We used Methotrexate (MTX) as a positive drug, which was obtained from Shanghai Sine Pharmaceutical Co., Ltd. (Shanghai, China) and its dosage was determined according to clinical routine usage.

2.3. Clinical assessment

To evaluate the severity of arthritis, clinical scores were daily detected by two independent and trained observers from the day of the second immunization. Arthritis index score was obtained on a scale of 0 to 4 for each limb. The detailed scoring standard was described in our previous reports (Qiu et al., 2018). The two hind limbs of rats were evaluated, resulting in a maximal score of 8 per animal. Simultaneously, the change in paw volume was determined by a volume displacement plethysmometer. In addition, the rats were daily weighed and the change in body weight was analyzed.

2.4. Measurement of serum biochemical parameters

At the end of the treatment experiment, the rats were euthanized, and their serum was collected to measure the levels of liver damage markers (AST, ALT) and indicators of renal function (Cre, BUN) using commercial kits from Jiancheng Bioengineering Institute (Nanjing, Jiangsu, China), following the manufacturer's instructions.

2.5. Radiographic assessment

To evaluate bone destruction in CIA rats, the left hind ankles and paws were collected for radiographic analysis. The degree of bone destruction was assessed using a scale of 0 to 3, based on our previously described method (Qiu et al., 2018; Liu et al., 2018). Radiographic scoring was conducted in a double-blind manner to minimize bias.

2.6. Histopathological evaluation

After radiographic analysis, the left ankles were immersed in an EDTA solution to remove calcium. Once the samples were soft enough to be penetrated by a needle without resistance, they were dehydrated, embedded, and sectioned into 4 μm thickness. The sections were stained with haematoxylin and eosin (H&E) and evaluated for histopathological changes including synovial hyperplasia, pannus formation, cartilage erosion, and bone destruction using a semi-quantitative scoring system based on our previous reports (Qiu et al., 2018; Liu et al., 2018).

2.7. Assessment of proinflammatory factors in joints

The right hind ankles and paws of rats were homogenized with cold phosphate buffer solution, as described in our previous reports (Qiu et al., 2018; Yu et al., 2021). TNFα and IL-1β in the joint homogenates were determined using the ELISA kits (SenBeiJia Bio-Tech, Nanjing, Jiangsu, China).

2.8. Cell culture

To obtain FLS cells, we isolated synovial tissues from the knee joints of CIA-Vehicle rats and digested them using a double enzymatic method with 0.25% trypsin and 0.4% type II collagenase, following the protocol described in our previous report (M. Liu et al., 2018; Z. Liu et al., 2018). The resulting cells were cultured in H-DMEM medium (Gibco, Grand Island, NY, USA) under standard conditions of 37 °C and 5% CO_2. In vitro experiments were conducted using cells from passages three to nine.

2.9. Cell viability assay

The FLS cells were incubated with Phil at concentrations ranging from 0 to 640 μM for 48 h, followed by the addition of MTS/PMS (Sigma, Saint Louis, MO, USA) and further incubation for 4 h. The absorbance was measured using a microplate reader at a wavelength of 490 nm.

2.10. Cell migration assay

When the cell monolayers reached 80% confluency, a sterile 200 μl pipette tip was used to create scratches. The cells were washed with PBS and treated with different concentrations of Phil for 4 h, then stimulated with 50 ng·ml^{-1} TNFα (Peprotech, Rocky Hill, NJ) for 24 h. The migration ratio of the cells was measured using Image J software (NIH, Bethesda, MD, United States).

2.11. Cell proliferation assay

The cells were pre-treated with 5 μM Phil for 4 h, stimulated with 50 ng·ml^{-1} TNFα for 24 h, and subsequently incubated with 10 μM EdU (KeyGen Biotech, Nanjing, Jiangsu, China) for 6 h. After fixation with methanol, the nuclei were stained with Hoechst 33342. The cell proliferation rate was determined by calculating the number of EdU-positive cells relative to the total number of Hoechst-positive cells.

2.12. Cell apoptosis assay

Flow cytometry was used to assess cell apoptosis. After treatment with different concentrations of Phil for 24 h, Annexin V-FITC and propidium iodide (PI) staining solutions (KeyGen Biotech, Nanjing, Jiangsu, China) were added to the cells, followed by analysis using flow cytometry (FACScan, Becton Dickinson).

2.13. Quantitative real-time PCR

The FLS cells were treated with different doses of Phil for 1 h and incubated with 50 ng·ml^{-1} TNFα for 24 h. TRIzol reagent (Invitrogen, Carlsbad, CA, USA) was added to the wells and total RNA was extracted. After reverse transcription with purified RNA and OligdT primers, real-time PCR was conducted using SYBR-Green qPCR Master Mixes (Vazyme Biotech, Jiangsu, China). The specific PCR primer pairs for TNFα, IL-6, IL-1β, MMP2, MMP9 and β-actin were utilized, as described previously (Qiu et al., 2018; Yu et al., 2021).

2.14. Western blot analysis

The FLSs were treated with different doses of Phil and then stimulated with 50 ng·ml^{-1} TNFα for 15 min. Radioimmuno-precipitation assay buffer was added to the wells and the supernatants were collected. The protein in the supernatants was separated using SDS-PAGE and transferred onto Polyvinylidene Fluoride membranes (PVDF, Millipore, Darmstadt, Germany). These PVDF membranes were blocked and then incubated with antibodies against p-p38, p-JNK, p-ERK, p38, JNK, ERK (Cell Signaling Technology, Beverly, MA, USA), IκBα and GAPDH (Santa Cruz Biotechnology, Dallas, CA, USA) overnight at 4 °C. Corresponding horseradish peroxidase-conjugated antibodies were used to incubate the membranes, and ECL detection reagent was added to visualize the bands. The relative expression was analyzed using Image J software.

2.15. Immunofluorescent staining

The cells were cultured and seeded onto glass cover slips in 24-well plates. Following that, they were fixed using methanol and permeabilized with 0.5% Triton-X 100. Subsequently, the cells were incubated with p65 antibody (Cell Signaling Technology, Beverly, MA, USA) and DAPI. Finally, the localization of p65 was observed using a Nikon A1R resonance scanning confocal microscope with a spectral detector (Nikon, Tokyo, Japan).

2.16. Statistics

The experiments were repeated at least three times unless otherwise indicated. For in vivo experiments, t-test was employed to compare the healthy control group and the CIA-Vehicle group, and one-way analysis of variance (ANOVA) was used to compare different treatment groups, followed by Tukey's post hoc analysis. The data are presented as the mean ± SEM. For in vitro experiments, t-tests were used to compare the TNFα-untreated group and the TNFα-treated but Phil-untreated group, and one-way ANOVA was

used to compare different Phil treatment groups, followed by Tukey's *post hoc* analysis. The data are presented as the mean ± SD. $P < 0.05$ was considered statistically significant.

3. Results

3.1. Synovitis and bone destruction of CIA rats were significantly attenuated by Phil treatment

To assess the therapeutic effect of Phil on RA, a rat model of CIA was established and different concentrations of Phil (10 and 20 mg·kg^{-1}) were intraperitoneally administrated daily for a period of 14 days (Fig. 1). The vehicle-treated group exhibited continuously increasing arthritis scores throughout the treatment period, with a maximum score of 8 (Fig. 2A and B). In contrast, Phil or MTX treatment effectively mitigated the development and progression of CIA (Fig. 2A and B). The changes in paw volume also reflected the efficacy of Phil or MTX in reducing arthritis symptoms (Fig. 2C). Notably, Phil exhibited greater anti-inflammatory potential than MTX, as evidenced by lower scores and paw volumes in Phil-treated CIA rats (Fig. 2A-C).

Bone destruction, a common feature of CIA animals, was analyzed by X-ray. As shown in Fig. 2D, compared with the normal controls, the hind paws of the vehicle-treated rats showed narrowed joint spacing, severe bone erosion, and rough bone surface. In contrast, Phil treatment significantly and dose-dependently inhibited bone destruction in CIA rats (Fig. 2D and 2E), indicating its potential anti-bone erosive action in RA.

To further investigate the inhibitory effect of Phil on arthritis severity, we performed a semi-quantitative histopathological assessment. Pathological features of RA, such as synovitis, pannus, and bone erosion, were clearly observed in the vehicle-treated CIA group. However, treatment with Phil effectively suppressed these pathological changes, resulting in significantly reduced histopathological scores (Fig. 3A and B).

A preliminary investigation was conducted to explore the potential side effects of Phil on CIA rats (Table 1). As expected, the body weight of the vehicle-treated CIA rats was significantly reduced. However, Phil treatment significantly and dose-dependently suppressed the loss of weight body. In addition, the liver and spleen indexes in the vehicle-treated group were significantly elevated, and this increase was inhibited by MTX or Phil treatment. No significant statistical differences were observed among the normal controls, vehicle-treated, MTX- or Phil-treated groups in terms of heart and kidney indexes, as well as levels of ALT, AST, Cre, and BUN. These preliminary data suggest that the doses of Phil employed in this study are unlikely to cause significant adverse side effects.

3.2. Production of pro-inflammatory cytokines in CIA animals was effectively reduced by Phil treatment

Inflammation is considered to be a key driver of RA pathogenesis. Considerable pro-inflammatory mediators, especially TNFα and IL-1β, are released and play pivotal roles in regulating the initiation and maintenance of joint inflammation (Vanderborgh et al., 2004; Polzer et al., 2010). Thus, the production of TNFα and IL-1β in the rat joint tissues was measured. In comparison to the normal controls, the vehicle-treated CIA rats had markedly increased levels of TNFα and IL-1β. However, these increases were significantly inhibited by Phil treatment in a dose-dependent manner (Fig. 4). These data suggested that anti-arthritic action of Phil might attribute, at least in part, to the decreased expression of pro-inflammatory factors.

3.3. Proliferation and migration of TNFα-induced arthritic FLSs were significantly suppressed by Phil treatment

To determine the possible cytotoxic effect of Phil in FLSs, an MTS assay was conducted. The result showed that Phil had little influence on the cell viability within the dose range of $0 \sim 640$ μM (Fig. 5A). In this study, no more than 10 μM Phil was used for *in vitro* experiments.

As is well known, the abnormal hyperplasia of synovial tissues in RA patients is caused by excessive proliferation of over-activated FLSs. Therefore, inhibiting the proliferation
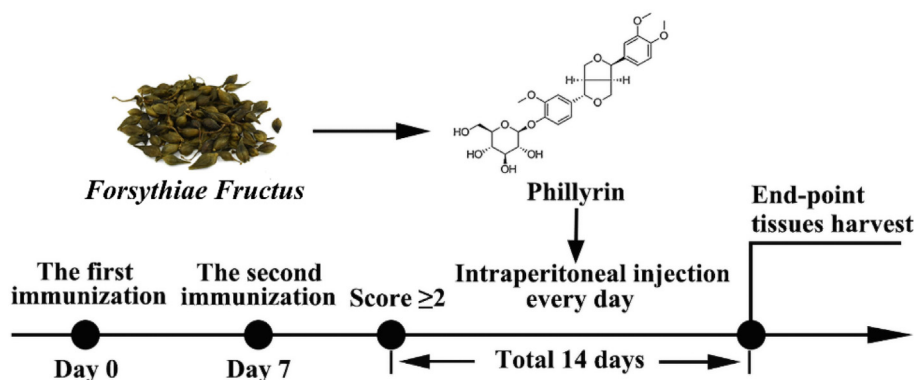
Fig. 1   The scheme of CIA induction and Phil's treatment. The rats received their first immunization on day 0, followed by a second immunization on day 7. Once their clinical score reached ≥ 2, CIA rats were randomly assigned to intraperitoneally receive either 10 mg·kg^{-1} or 20 mg·kg^{-1} of Phillyrin or vehicle (0.9% saline) daily for 14 days. Additionally, the positive drug group was given 3 mg·kg^{-1} of MTX once every 3 days. After 14 days of treatment, the rats were sacrificed and their tissues were collected for further analysis.
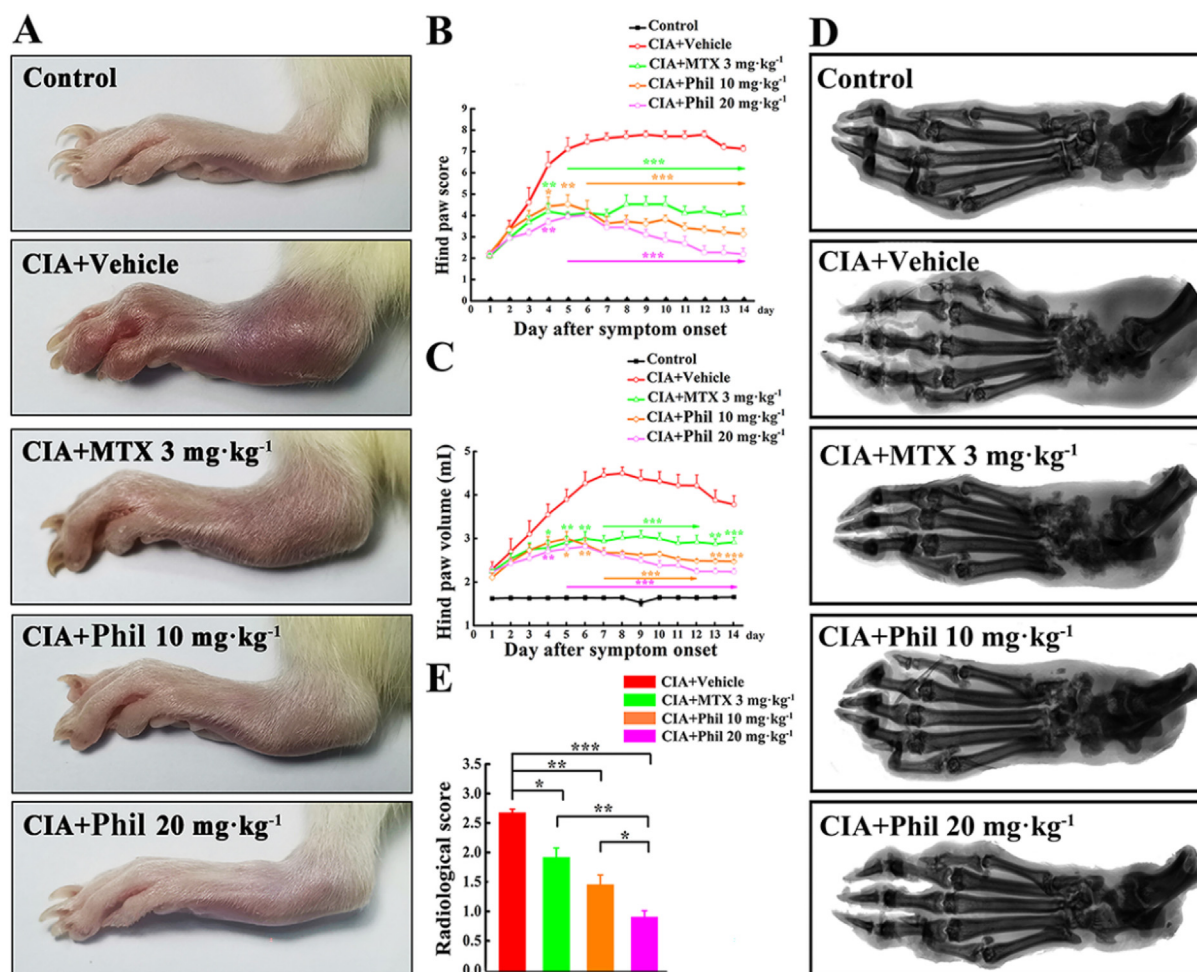
Fig. 2   Phil significantly improves the symptoms in the rats with CIA. (A) At the end of the treatment, photographs of the hind paws of the rats with CIA were taken. Hind paw score **(B)** and Hind paw volume **(C)** were assessed during the treatment period (mean $\pm$ SEM, n = 7, *$P < 0.05$, **$P < 0.01$ and ***$P < 0.001$ versus CIA-Vehicle group); Representative radiographs of hind paws from different groups were shown in **(D)**, and **(E)** the radiological scoring scale was used to score the different groups (mean $\pm$ SEM, n = 7, *$P < 0.05$, **$P < 0.01$ and ***$P < 0.001$).

of FLSs is considered as a promising strategy for the treatment of RA. In our study, the EdU incorporation results suggested that the proliferation rate of FLSs was markedly enhanced upon TNFα stimulation. But the enhancement was effectively suppressed by 5 μM Phil (Fig. 5B and 5C).

Migration of FLSs to cartilage and bone is a critical step in the deterioration of RA, therefore, suppressing FLSs' migration is an important approach to prevent the destructive progress of this disease. Our wound healing results showed that Phil could significantly inhibit TNFα-stimulated migration at concentrations greater than 1 μM (Fig. 5D and E). Additionally, we also examined the apoptotic inducing effect of Phil using flow cytometry and found that Phil did not affect the apoptosis of FLSs at the given doses (Fig. 5F).

3.4. The transcripts of inflammatory cytokines and MMP-9 in arthritic FLSs were suppressed by Phil treatment

We demonstrated that Phil could play an anti-inflammatory role in CIA rats. To further confirm this inhibitory effect, we used real-time PCR to detect the mRNA expression of multi-

ple pro-inflammatory factors, including *TNFα*, *IL-1β*, *IL-6*, and *IL-8*. The results showed that TNFα stimulated the up-regulation of these inflammatory mediators, while Phil treatment significantly decreased their expression. RA FLSs contribute to the degradation of connective tissue by secreting substantial amounts of MMPs, which leads to the breakdown of cartilage. The real-time PCR data from our study showed that Phil had no significant effect on the expression of *MMP-2*, but effectively inhibited the production of *MMP-9* (Fig. 6).

3.5. Phil treatment blocked TNFα-induced activations of NF-κB and MAPKs

To explore the mechanisms underlying Phil's inhibition on FLS cells, TNFα-stimulated activation of MAPKs was examined in arthritic FLSs with or without Phil treatment. As shown in Fig. 7A and 7B, the phosphorylation levels of p38, JNK, and ERK were markedly up-regulated in TNFα-induced FLSs. However, all these up-regulations were clearly blocked by Phil treatment (Fig. 7A and 7B). In addition to
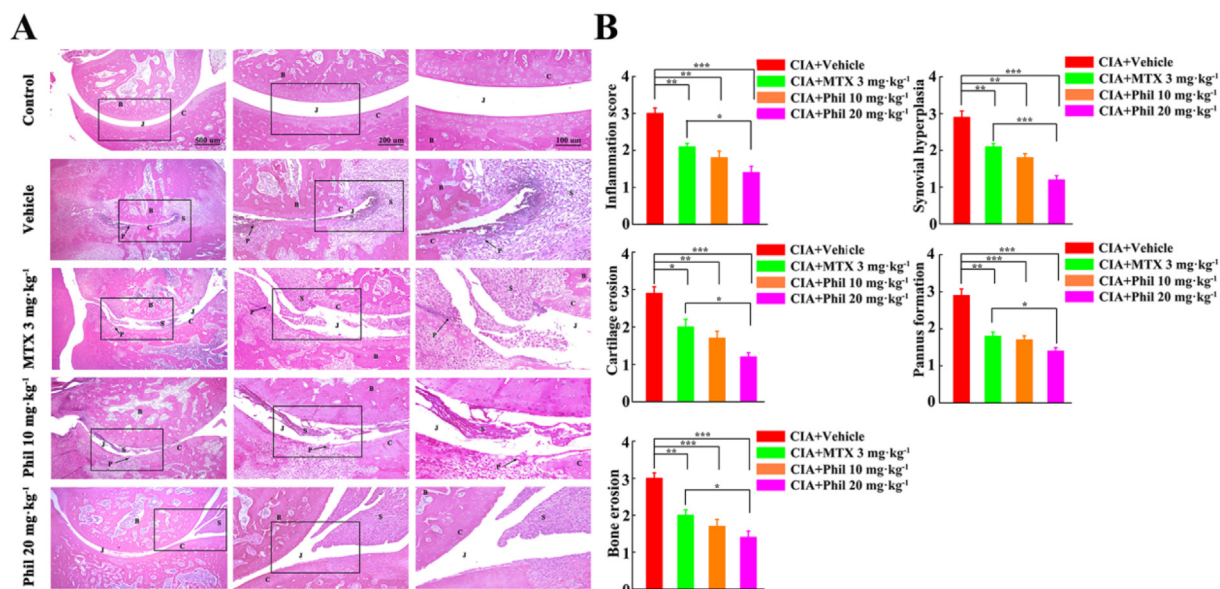
Fig. 3   Phil significantly ameliorates the pathological changes in the rats with CIA. (A) Representative H&E staining of ankle joints in different groups. **(B)** Histopathological evaluation of ankle joints in different groups. (mean ± SEM, n = 7, *$P < 0.05$, **$P < 0.01$ and ***$P < 0.001$). B, bone; C, cartilage; J, joint space; P, pannus; S, synovium.

Table 1   Changes in body weight, organ indexes, and blood biochemical parameters of rats receiving various treatments.

Parameters	Control	Vehicle	MTX (3 mg·kg^{-1})	Phil (10 mg·kg^{-1})	Phil (20 mg·kg^{-1})
Body weight gain (%)	10.21 ± 0.95	−6.81 ± 0.76[###]	3.37 ± 0.69[***]	3.55 ± 0.76[***]	5.59 ± 0.71[***]
Heart index (mg/g)	0.3 ± 0.01	0.37 ± 0.02	0.35 ± 0.01	0.29 ± 0.01	0.36 ± 0.01
Liver index (mg/g)	2.82 ± 0.11	3.66 ± 0.16[##]	3.21 ± 0.06[*]	3.43 ± 0.08	3.12 ± 0.09[*]
Spleen index (mg/g)	0.22 ± 0.01	0.41 ± 0.02[###]	0.29 ± 0.02[***]	0.34 ± 0.02[*]	0.29 ± 0.02[***]
Kidney index (mg/g)	0.78 ± 0.02	0.84 ± 0.02	0.76 ± 0.02	0.81 ± 0.03	0.84 ± 0.04
AST (U/L)	21.59 ± 1.07	24.47 ± 1.48	24.16 ± 0.92	23.7 ± 1.3	21.18 ± 1.19
ALT (U/L)	4.75 ± 0.16	4.91 ± 0.15	3.97 ± 0.5	4.17 ± 0.59	4.03 ± 0.18
Cre (mmol/L)	32.9 ± 1.77	34.71 ± 1.72	35.14 ± 1.52	33.51 ± 2.12	33.65 ± 1.22
BUN (mmol/L)	7.56 ± 0.59	7.88 ± 0.79	7.92 ± 0.42	8.21 ± 0.44	7.39 ± 0.15

After 14 days of treatment, the body weight, organ indexes, and levels of AST, ALT, Cre, and BUN were assessed in rats from different groups (mean ± SEM, n = 7, [##]$P < 0.05$ and [###]$P < 0.001$ versus normal control; *$P < 0.05$ and ***$P < 0.001$ versus vehicle group).
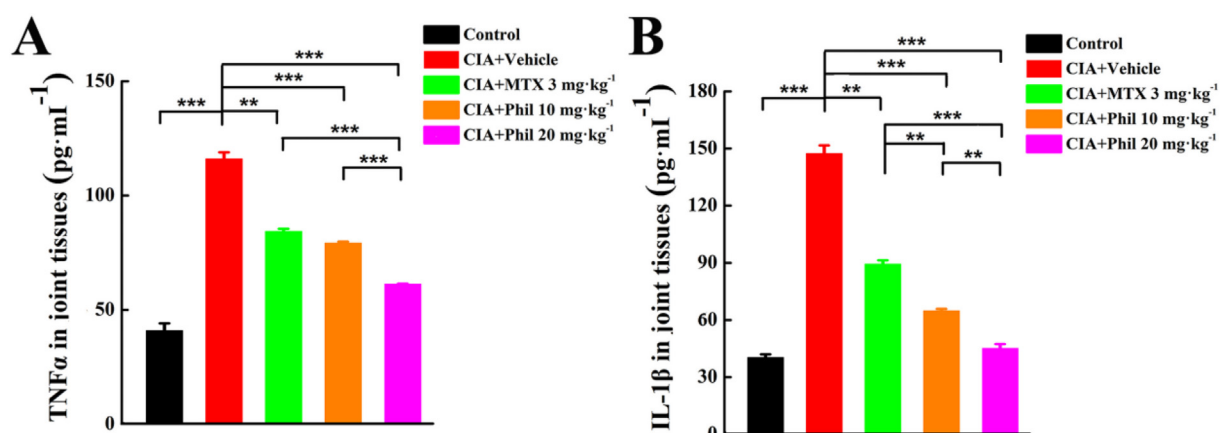
Fig. 4   Phil significantly decreases the production of inflammatory cytokines (TNFα and IL-1β) in the joint tissues of the rats with CIA. After homogenizing the right hind ankles and paws of CIA rats, the levels of TNFα **(A)** and IL-1β **(B)** were quantified (means ± SEM, n = 7, **$P < 0.01$ and ***$P < 0.001$).
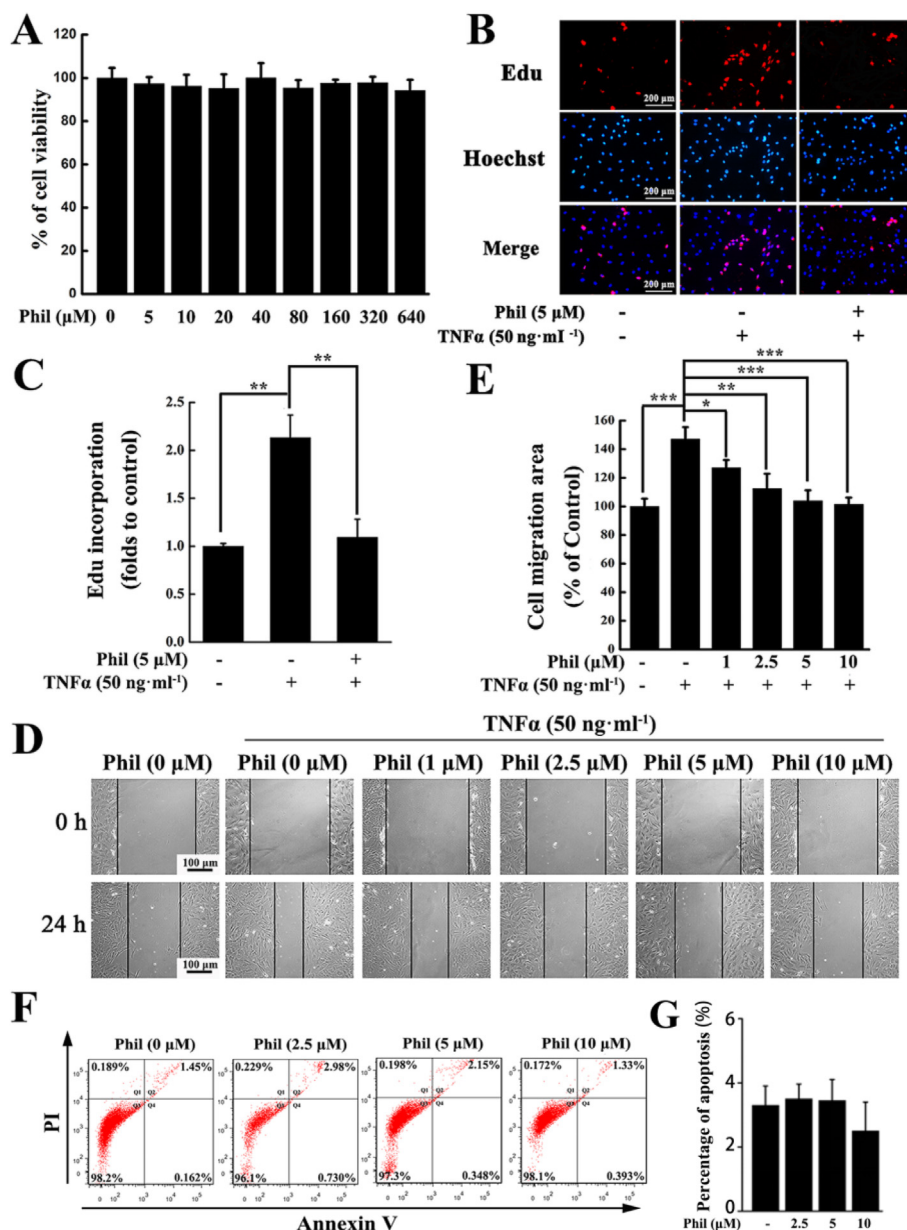
Fig. 5 **Phil treatment suppresses the proliferation and migration of arthritic FLS cells stimulated by TNFα. (A)** MTS assay proved that Phil at given doses had little effect on the arthritic FLSs' viability (means ± SD, n = 3). **(B, C)** EdU incorporation assay proved that 5 μM Phil could reduce the proliferation rate of arthritic FLSs. Data are presented as means ± SD of three independent experiments (**$P < 0.01$**). **(D, E)** Representative graphs and statistical analysis of the wound healing assay (means ± SD, three independent experiments, *$P < 0.05$, **$P < 0.01$ and ***$P < 0.001$). **(F)** Representative graphs and statistical analysis of the apoptosis assay (means ± SD, three independent experiments).

MAPKs, we also evaluated the activation of NF-κB pathway, which plays a crucial role in the pathogenesis of RA (Li and Makarov, 2006). As shown in Fig. 7C and D, TNFα stimulation caused a significant degradation of IκBα, an inhibitor of NF-κB. however, Phil treatment dose-dependently inhibited this degradation process. In consistency with these data of Western blot, the results of immunofluorescent staining showed that Phil effectively blocked the nuclear translocation of p65 (Fig. 7E), further confirming the inhibition of Phil on the TNFα-induced NF-κB pathway.

4. Discussion

In this study, we provided convincing evidence that Phil could effectively inhibit synovitis and bone erosion in CIA rats. This suppressive action of Phil might be involved in the amelioration of pathogenic characteristic of arthritic FLSs by blocking NF-κB and MAPKs signaling pathways.

Intensive inflammation is the most distinctive feature of RA (Polzer et al., 2010; Smolen et al., 2005). Inhibiting the synthesis of inflammatory cytokines to effectively control
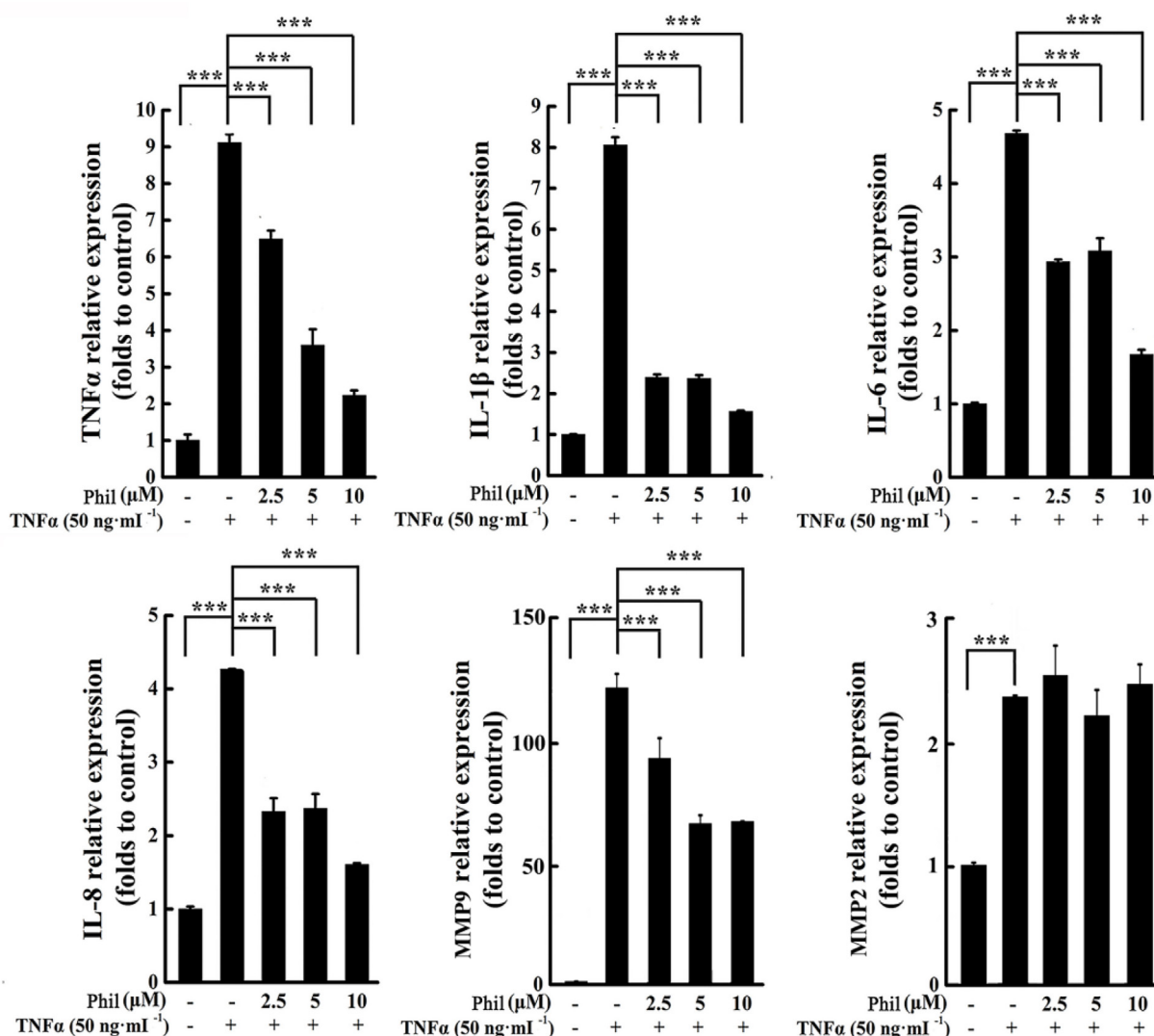
Fig. 6   Phil treatment suppresses the transcripts of inflammatory cytokines and MMP9 in TNFα-induced arthritic FLSs. FLS cells were treated with Phil for 1 h, followed by stimulation with TNFα for 24 h. Real-time PCR was then utilized to assess the mRNA expression of various inflammatory cytokines (*IL-1β*, *IL-6*, *IL-8*, and *TNFα*) and MMPs (*MMP2* and *MMP9*). Data are presented as means ± SD of three independent experiments (***$P < 0.001$).

inflammation is an important strategy for RA treatment. (Smolen and Aletaha, 2015; Schett et al., 2020). In this study, The results of clinical scoring, paw volume measurement, and histopathological assessment all indicated that Phil was effective in reducing the inflammatory responses in CIA rats. In addition, the ELISA results showed that the levels of pro-inflammatory factors in joint tissues were decreased by Phil. In consistence with the *in vivo* findings, the *in vitro* data suggested that Phil treatment dramatically reduced the transcripts of inflammatory mediators including *IL-1β*, *IL-6*, *IL-8*, and *TNFα* in arthritic FLSs induced by TNFα. Apart from inflammatory cytokines, we also investigated the impact of Phil on the expression of MMP2 and MMP9. As is well known, MMPs, particularly MMP-2 and MMP-9, play a crucial role in breaking down the extracellular matrix and degrading tissues (Gruber et al., 1996; Tchetverikov et al., 2004). While MMP-2 is constitutively expressed in an inactive form in various cell types, MMP-9 can be induced by inflammatory

cytokines, indicating a close association with synovial inflammation (Giannelli et al., 2004). Our study found that Phil had little effect on MMP-2 production, but significantly inhibited the synthesis of MMP-9. These results were consistent with our *in vivo* findings, which showed that Phil had a protective effect against cartilage erosion. Phil's ability to simultaneously down-regulate multiple pro-inflammatory mediators and MMP9 distinguishes it from single-mediator-targeted therapies such as biological agents, and may provide therapeutic advantages in the treatment of RA.

Since bone erosion is tightly related to functional disability, blocking progressive joint destruction is a crucial and challenging goal of RA treatment. In the present study, the radiographic analysis suggested that Phil treatment significantly suppressed bone erosion in CIA rats, which was further confirmed by the result of the histopathological assessment. As is well known, osteoclasts are specialized bone-resorbing cells that play a critical role in bone destruction, and their
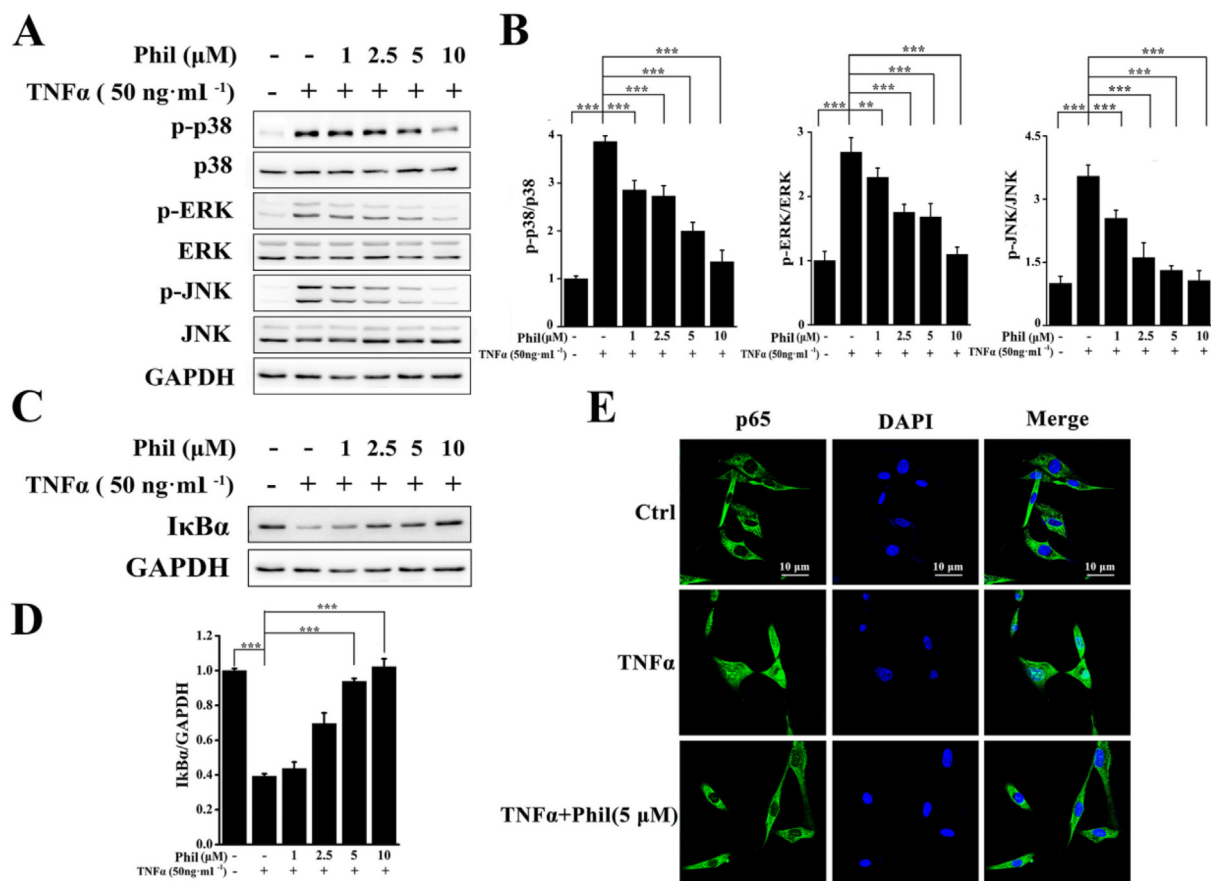
Fig. 7   Phil inhibits the activations of MAPKs and NF-κB in TNFα-stimulated arthritic FLS cells. (A and C) FLS cells were treated with Phil at the specified doses for 1 h, followed by stimulation with TNFα for 15 min. Western blot was used to detect the activation of MAPK and NF-κB using the indicated antibodies. **(B and D)** The relative expressions of p-p38, p-ERK, p-JNK and IκBα were determined by densitometric analysis using Image J. (means ± SD, three independent experiments, $**P < 0.01$ and $***P < 0.001$). **(E)** FLS cells were treated with 5 μM Phil for 4 h, followed by stimulation with 50 ng·ml^{-1} TNFα for 30 min. Representative laser confocal images demonstrated that Phil inhibited the nuclear translocation of p65.

formation and activation can be triggered and promoted by inflammation (Danks et al., 2016; Tateiwa et al., 2019). In our study, Phil showed a strong anti-inflammatory potential by down-regulating the synthesis of multiple inflammatory mediators. Thus, it was highly possible that Phil suppressed bone erosion in CIA rats through an indirect effect of anti-inflammation. However, our previous study demonstrated that Phil could inhibit RANKL-induced osteoclast formation and prevent LPS-Induced osteolysis in mice (Wang et al., 2019). Taken together, Phil might exert a synergistic effect on anti-bone erosion by indirectly suppressing inflammatory response and directly inhibiting osteoclast formation.

Our data proved that Phil possesses anti-arthritic potential, which may be attributed to its ability to inhibit the activation of NF-κB and MAPKs. NF-κB is an essential intracellular nuclear transcription factor which is involved in inflammatory and immune responses, and its activation is essential for the pathogenesis of RA by increasing the relative expressions of inflammatory factors such as *IL-1β*, *IL-6*, and *TNFα*. This increased expression of pro-inflammatory genes leads to further activation of NF-κB, thereby amplifying the inflammatory response. Its continued activation was observed in synovial tissues from RA patients and animal models of arthritis (Coste et al., 2015; Li and Makarov, 2006). Thus, NF-κB is an effective target molecule for RA treatment. In this study, the degradation of IκBα and the nuclear translocation of NF-κB p65 induced by TNFα were obviously inhibited by Phil. The down-regulation of relative expressions of NF-κB target genes including *TNFα*, *IL-1β*, *IL-6*, and *IL-8* further confirmed the inhibitory effect of Phil on NF-κB pathway in TNFα-induced FLSs. Besides NF-κB, Phil could also decrease the phosphorylations of the MAPK family members (ERK, JNK, and p38), which have also been shown to be indispensable in the pathological process of RA (Schett et al., 2008; Coste et al., 2015). The capacity of Phil to block the activations of all these three kinases indicated that Phil might target a common activating kinase or deactivating phosphatase. In addition to the NF-κB and MAPK pathways, other signaling pathways, such as JAK/STAT and PI3K/AKT, have also been shown to play significant roles in RA pathogenesis (Song et al., 2019; Simon et al., 2020). Recently, phillyrin was reported as a novel inhibitor of cyclic AMP phosphodiesterase 4, which is a promising target for the treatment of RA (Li et al., 2018; Nishibe et al., 2021). Therefore, further investigations are

necessary to fully understand the comprehensive molecular mechanisms underlying Phil's anti-RA effects and its direct targets.

In summary, our study provided evidence for Phil's therapeutic potential in treating CIA rats *in vivo* and its ability to suppress pathogenic properties of arthritic FLS by inhibiting NF-κB and MAPKs signaling pathways *in vitro*. These data strongly suggest that Phil has the potential to be developed into a novel anti-RA agent.

CRediT authorship contribution statement

Gang Chen: Methodology, Validation, Investigation, Formal analysis, Writing – original draft, Visualization. **Yuhang Mao:** Investigation, Validation, Formal analysis. **Jing Wang:** Investigation, Methodology. **Junnan Zhou:** Methodology, Visualization. **Li Diao:** Visualization. **Sirui Wang:** Visualization. **Wenjuan Zhao:** Investigation. **Xinyi Zhu:** Investigation. **Xiaolu Yu:** Validation. **Fuli Zhao:** Validation. **Xuan Liu:** Investigation. **Mei Liu:** Conceptualization, Writing – review & editing, Supervision, Project administration, Funding acquisition.

Data availability statement.

The datasets generated and/or analyzed in the current study are available from the first author and the corresponding author upon reasonable request.

Declaration of Competing Interest

The authors declare that they have no known competing financial interests or personal relationships that could have appeared to influence the work reported in this paper.

Acknowledgment

References

Cheng, Y., Liang, X., Feng, L., Liu, D., Qin, M., Liu, S., Liu, G., Dong, M., 2017. Effects of phillyrin and forsythoside a on rat cytochrome p450 activities in vivo and in vitro. Xenobiotica. 47 (4), 297–303. https://doi.org/10.1080/00498254.2016.1193262.

Coste, E., Greig, I.R., Mollat, P., Rose, L., Gray, M., Ralston, S.H., Hof, R., 2015. Identification of small molecule inhibitors of RANKL and TNF signalling as anti-inflammatory and antiresorptive agents in mice. Ann. Rheum. Dis. 74 (1), 220–226. https://doi.org/10.1136/annrheumdis-2013-203700.

Danks, L., Komatsu, N., Guerrini, M., Sawa, S., Armaka, M., Kollias, G., Nakashima, T., Takayanagi, H., 2016. RANKL expressed on synovial fibroblasts is primarily responsible for bone erosions during joint inflammation. Ann. Rheum. Dis. 75 (6), 1187–1195. https://doi.org/10.1136/annrheumdis-2014-207137.

Du, Y., You, L., Ni, B., Na, S., Ni, J., 2020. Phillyrin Mitigates Apoptosis and Oxidative Stress in Hydrogen Peroxide-Treated RPE Cells through Activation of the Nrf2 Signaling Pathway. Oxid

Med Cell Longev. 1–16, 2020. https://doi.org/10.1155/2020/2684672.

Giannelli, G., Erriquez, R., Iannone, F., Marinosci, F., Lapadula, G., Antonaci, S., 2004. MMP-2, MMP-9, TIMP-1 and TIMP-2 levels in patients with rheumatoid arthritis and psoriatic arthritis. Clin Exp Rheumatol 22 (3), 335–338. PMID: 15144129.

Gruber, B.L., Sorbi, D., French, D.L., Marchese, M.J., Nuovo, G.J., Kew, R.R., Arbeit, L.A., 1996. Markedly elevated serum MMP-9 (gelatinase B) levels in rheumatoid arthritis: a potentially useful laboratory marker. Clin Immunol Immunopathol 78 (2), 161–171. https://doi.org/10.1006/clin.1996.0025.

Khraishi, M.M., 2014. Experience with subcutaneous abatacept for rheumatoid arthritis: an update for clinicians. Ther. Adv. Musculoskelet. Dis. 6 (5), 159–168. https://doi.org/10.1177/1759720X14551567.

Klareskog, L., Catrina, A.I., Paget, S., 2009. Rheumatoid arthritis. Lancet 373, 659–672. https://doi.org/10.1016/S0140-6736(09)60008-8.

Laragione, T., Brenner, M., Mello, A., Symons, M., Gulko, P.S., 2010. The arthritis severity locus Cia5d is a novel genetic regulator of the invasive properties of synovial fibroblasts. Arthritis Rheumatol. 58 (8), 2296–2306. https://doi.org/10.1002/art.23610.

Li, X., Makarov, S.S., 2006. An essential role of NF-kappaB in the "tumor-like" phenotype of arthritic synoviocytes. Proc. Natl. Acad. Sci. 103 (46), 17432–17437. https://doi.org/10.1073/pnas.0607939103.

Li, H., Zuo, J., Tang, W., 2018. Phosphodiesterase-4 Inhibitors for the Treatment of Inflammatory Diseases. Front. Pharmacol. 9, 1048. https://doi.org/10.3389/fphar.2018.01048.

Liu, Z., Zhou, L., Ma, X., Sun, S., Qiu, H., Li, H., Xu, J., Liu, M., 2018. Inhibitory effects of tubeimoside I on synoviocytes and collagen-induced arthritis in rats. J Cell Physiol. 233 (11), 8740–8753. https://doi.org/10.1002/jcp.26754.

Liu, M., Zhou, X., Zhou, L., Liu, Z., Yuan, J., Cheng, J., Zhao, J., Wu, L., Li, H., Qiu, H., Xu, J., 2018. Carnosic acid inhibits inflammation response and joint destruction on osteoclasts, fibroblast-like synoviocytes, and collagen-induced arthritis rats. J Cell Physiol 233 (8), 6291–6303. https://doi.org/10.1002/jcp.26517.

Lu, Z., Cao, H., Liu, D., Zheng, Y., Yu, L., 2020. Optimal combination of anti-inflammatory components from Chinese medicinal formula Liang-Ge-San. J. Ethnopharmacol. 269,. https://doi.org/10.1016/j.jep.2020.113747 113747.

Müller-Ladner, U., Pap, T., Gay, R.E., Neidhart, M., Gay, S., 2005. Mechanisms of disease: the molecular and cellular basis of joint destruction in rheumatoid arthritis. Nat Clin Pract Rheumatol. 1 (2), 102–110. https://doi.org/10.1038/ncprheum0047.

Nishibe, S., Mitsui-Saitoh, K., Sakai, J., Fujikawa, T., 2021. The biological effects of forsythia leaves containing the cyclic AMP Phosphodiesterase 4 inhibitor Phillyrin. Molecules. 26 (8), 2362. https://doi.org/10.3390/molecules26082362.

Noss, E.H., Chang, S.K., Watts, G., Brenner, M.B., 2011. Cadherin-11 engagement modulates matrix metalloproteinase production by rheumatoid arthritis synovial fibroblasts. Arthritis & Rheumatism. 63, 3768–3778. https://doi.org/10.1002/art.30630.

O'Dell, J.R., 2004. Therapeutic strategies for rheumatoid arthritis. New Engl. J. Med. 350, 2591–2602. https://doi.org/10.1056/NEJMra040226.

Pallavi, B., Kyle, J., 2019. Regulation of fibroblast-like synoviocyte transformation by transcription factors in arthritic diseases. Biochem. Pharmacol. 165, 145–151. https://doi.org/10.1016/j.bcp.2019.03.018.

Pharmacopoeia Commission of PRC. Pharmacopoeia of the People' s Republic of China, 2015 ed. China Medical Science Press, Beijing. 2015. https://scholar.google.com/scholar?q = Pharmacopoeia.

Polzer, K., Joosten, L., Gasser, J., Distler, J.H., Ruiz, G., Baum, W., 2010. Interleukin-1 is essential for systemic inflammatory bone loss.

Ann. Rheum. Dis. 69 (1), 284–290. https://doi.org/10.1136/ard.2008.104786.

Putte, L.B., Rau, R., Breedveld, F.C., Kalden, J.R., Malaise, M.G., Riel, P.L., Schattenkirchner, M., Emery, P., Burmester, G.R., Zeidler, H., Moutsopoulos, H.M., Beck, K., Kupper, H., 2003. Efficacy and safety of the fully human anti-tumour necrosis factor alpha monoclonal antibody adalimumab (D2E7) in DMARD refractory patients with rheumatoid arthritis: a 12 week, phase II study. Ann. Rheum. Dis. 62, 68–77. https://doi.org/10.1136/ard.2003.009563.

Qiu, H., Sun, S., Ma, X., Cui, C., Chen, G., Liu, Z., Li, H., Liu, M., 2018. Jatrorrhizine hydrochloride suppresses proliferation, migration, and secretion of synoviocytes in vitro and ameliorates rat models of rheumatoid arthritis in vivo. Int. J. Mol. Sci. 19 (5), 1514. https://doi.org/10.3390/ijms19051514.

Qu, H., Zhang, Y., Yan, W., Li, B., Sun, W., 2010. Antioxidant and antibacterial activity of two compounds (forsythiaside and forsythin) isolated from forsythia suspensa. J. Pharm. Pharmacol. 60 (2), 261–266. https://doi.org/10.1211/jpp.60.2.0016.

Ralph, J.A., Morand, E.F., 2008. MAPK phosphatases as novel targets for rheumatoid arthritis. Expert. Opin. Ther. Tar. 12 (7), 795–808. https://doi.org/10.1517/14728222.12.7.795.

Schett, G., Zwerina, J., Firestein, G., 2008. The p38 mitogen-activated protein kinase (MAPK) pathway in rheumatoid arthritis. Ann. Rheum. Dis. 67 (7), 909–916. https://doi.org/10.1136/ard.2007.074278.

Schett, G., Tanaka, Y., Isaacs, J.D., 2020. Why remission is not enough: underlying disease mechanisms in RA that prevent cure. Nat. Rev. Rheumatol. 17, 135–144. https://doi.org/10.1038/s41584-020-00543-5.

Scott, D.L., 2012. Biologics-based therapy for the treatment of rheumatoid arthritis. Clin. Pharmacol. Ther. 9 (1), 30–43. https://doi.org/10.1038/clpt.2011.278.

Simon, L.S., Taylor, P.C., Choy, E.H., Sebba, A., Quebe, A., Knopp, K.L., Porreca, F., 2020. The Jak/STAT pathway: a focus on pain in rheumatoid arthritis. Semin Arthritis Rheum. 51 (1), 278–284. https://doi.org/10.1016/j.semarthrit.2020.10.008.

Smolen, J.S., Aletaha, D., 2015. Rheumatoid arthritis therapy reappraisal: strategies, opportunities and challenges. Nat. Rev. Rheumatol. 11 (5), 276–289. https://doi.org/10.1038/nrrheum.2015.8.

Smolen, J.S., Redlich, K., Zwerina, J., Aletaha, D., Steiner, G., Schett, G., 2005. Pro-inflammatory cytokines in rheumatoid arthritis. Clin. Rev. Allerg. Immu. 28, 239. https://doi.org/10.1385/CRIAI:28:3:239.

Song, B., Li, X.F., Yao, Y., Xu, Q.Q., Meng, X.M., Huang, C., Li, J., 2019. BMP9 inhibits the proliferation and migration of fibroblast-like synoviocytes in rheumatoid arthritis via the PI3K/AKT signaling pathway. Int Immunopharmacol. 74,. https://doi.org/10.1016/j.intimp.2019.105685 105685.

Tateiwa, D., Yoshikawa, H., Kaito, T., 2019. Cartilage and bone destruction in arthritis: pathogenesis and treatment strategy: a literature review. Cells. 8 (8), 818. https://doi.org/10.3390/cells8080818.

Tchetverikov, I., Ronday, H.K., Van El, B., Kiers, G.H., Verzijl, N., TeKoppele, J.M., Huizinga, T.W., DeGroot, J., Hanemaaijer, R., 2004. MMP profile in paired serum and synovial fluid samples of patients with rheumatoid arthritis. Annals of the rheumatic diseases 63 (7), 881–883. https://doi.org/10.1136/ard.2003.013243.

Tolboom, T., Helm, V., Nelissen, R., Breedveld, F.C., Toes, R., Huizinga, T., 2005. Invasiveness of fibroblast-like synoviocytes is an individual patient characteristic associated with the rate of joint destruction in patients with rheumatoid arthritis. Arthritis Rheumatism. 52 (7), 1999–2002. https://doi.org/10.1002/art.21118.

Vanderborght, A., Linsen, L., Thewissen, M., Geusens, P., Raus, J., Stinissen, P., 2004. Osteoprotegerin and receptor activator of nuclear factor-kappaB ligand mRNA expression in patients with rheumatoid arthritis and healthy controls. J. Rheumatol. 31 (8), 1483–1490 http://europepmc.org/article/MED/15290725.

Wang, J., Chen, G., Zhang, Q., Zhao, F., Liu, M., 2019. Phillyrin attenuates osteoclast formation and function and prevents LPS-induced osteolysis in mice. Front. Pharmacol. 10, 1188–1202. https://doi.org/10.3389/fphar.2019.01188.

Wang, Z., Xia, Q., Liu, X., Liu, W., Huang, W., Mei, X., Luo, J., Shan, M., Lin, R., Zou, D., Ma, Z., 2018. Phytochemistry, pharmacology, quality control and future research of Forsythia suspensa (Thunb.) Vahl: a review. J. Ethnopharmacol. 210, 318–339. https://doi.org/10.1016/j.jep.2017.08.040.

Yang, L., Zhou, X., Huang, W., Fang, Q., Hu, J., Yu, L., Ma, N., Zhang, W., 2017. Protective effect of phillyrin on lethal LPS-induced neutrophil inflammation in zebrafish. Cell. Physiol. Biochem. 43 (5), 2074–2087. https://doi.org/10.1159/000484192.

Yu, X., Zhou, J., Zhao, F., Liu, X., Mao, Y., Diao, L., Wen, C., Liu, M., 2021. Tomatidine suppresses the destructive behaviors of fibroblast-like synoviocytes and ameliorates Type II collagen-induced arthritis in rats. Front. Pharmacol. 12,. https://doi.org/10.3389/fphar.2021.670707 670707.

Zhang, F., Li, Z., Yang, X., Xie, Z., Dai, Y., 2020. Discovery of anti-flu substances and mechanism of Shuang-Huang-Lian water extract based on serum pharmaco-chemistry and network pharmacology. J. Ethnopharmacol. 268,. https://doi.org/10.1016/j.jep.2020.113660 113660.

Zhang, D., Qi, B., Li, D., Feng, J., Liu, X., 2019. Phillyrin relieves lipopolysaccharide-induced AKI by protecting against glycocalyx damage and inhibiting inflammatory responses. Inflammation 43 (2), 1–12. https://doi.org/10.1007/s10753-019-01136-5.

Zhang, W., Zhu, L., Jiang, J., 2014. Active ingredients from natural botanicals in the treatment of obesity. Obes. Rev. 15 (12), 957–967. https://doi.org/10.1111/obr.12228.

Zhong, W.T., Wu, Y.C., Xie, X.X., Zhou, X., Wei, M.M., Soromou, L.W., Ci, X.X., Wang, D.C., 2013. Phillyrin attenuates LPS-induced pulmonary inflammation via suppression of MAPK and NF-κB activation in acute lung injury mice. Fitoterapia. 90, 132–139. https://doi.org/10.1016/j.fitote.2013.06.003.

Zhou, Y., Toh, M.L., Zrioual, S., Miossec, P., 2007. IL-17A versus IL-17F induced intracellular signal transduction pathways and modulation by IL-17RA and IL-17RC RNA interference in AGS gastric adenocarcinoma cells. Cytokine. 38 (3), 157–164. https://doi.org/10.1016/j.cyto.2007.06.002.